Solvent and Solvent Density Effects on the Spectral Shifts and the Bandwidths of the Absorption and the Resonance Raman Spectra of Phenol Blue

T. Yamaguchi, Y. Kimura,* and N. Hirota*

Department of Chemistry, Graduate School of Science, Kyoto University, Kyoto 606-01, Japan

Received: April 16, 1997; In Final Form: September 18, 1997[⊗]

We have measured the absorption and the resonance Raman spectra of a solvatochromic dye, phenol blue, in liquid and supercritical solvents. We have found anomalous solvent dependence of the absorption bandwidth in liquid solvents: the width has apparently no correlation with the absorption peak shift. On the other hand, we have found good linear correlation between the absorption peak shift and the peak position of the resonance Raman bands (the C═N and the C═O stretching modes). The relative intensities of the Raman bands and the bandwidth of the C═N stretching mode also show correlation with the absorption peak shift. Incorporating these Raman data, the anomalous bandwidth of the absorption spectrum is explained by the change of the intramolecular vibrational contribution to the absorption bandwidth due to the electronic structure change by the solvent, which cancels the change of the solvent contribution. We have estimated the solvent reorganization energy assuming linear dependence of the intramolecular contribution on the absorption band center and neglecting the solvent reorganization energy in alkanes such as ethane and cyclohexane. In liquid solution, the estimated solvent reorganization energy is correlated fairly well with the absorption peak shift. Solvent dependence of the Raman bandwidth of the C═N stretching mode resembles the solvent dependence of the solvent reorganization energy estimated in this way. Relatively large bandwidths of both absorption and resonance Raman spectra have been observed in supercritical solvents compared with those in liquid solvents of a similar absorption peak shift. We interpreted this as due to the small refractive indices of the supercritical solvents relative to the liquid solvents; the large refractive indices of the liquid solvents only make the absorption peak shifts without broadening the absorption spectra.

1. Introduction

In chemical processes in solution, solvents play such an important role that we can hardly neglect.[1] For example, the mean potential by solvent molecules changes the chemical potential of a solute dissolved in solvent, and sometimes even its electronic structure. The thermal fluctuation of the solvent mean potential is also quite important, since it reveals itself in the electron transfer reaction, the energy relaxation, the isomerization, and so on. Spectroscopic methods are powerful tools to study such solvent effects. The spectrum in solution is different from that in the gas phase, not only in its peak position but also in its width. The peak shift is the transition energy shift due to the solvent mean potential. The broadening is induced by the solvent fluctuation, and we can extract from them the information on the static and dynamical fluctuation of solvents by proper treatments.

Solvent effects on the absorption peak shift (solvatochromism) and the fluorescence peak shift have long attracted much attention. There have been many theoretical and experimental studies performed to reveal the relation between the solvent properties and the solvatochromic shifts.[1] Most theoretical treatments are based on the continuum model of the solvent, and calculate the effect of the reaction field on the energy difference between the ground and the excited states. These theories sometimes succeed in correlating the shift with the solvent properties such as the dielectric constant, but sometimes fail. In application, the solvent shift itself is used as an indicator of the solvent property as is represented by the π^*-value or the E_T value.

In contrast to the extensive studies on the peak shift, the study on the absorption bandwidth is now under development. Recently intensive studies were performed on the absorption and the fluorescence band shapes in connection with electron-transfer reactions to extract the reaction free energies and solvent reorganization energies, which are important parameters in electron-transfer reactions.[2−9] The theoretical treatments on the solvent fluctuation have been in many cases based on the dielectric continuum model, as in the case of the spectral shift. As for the solvent reorganization, only the reorientation of the dipole moments of solvents is considered in this model. Recently the importance of the reorientation of multipole moments and translational motions was both experimentally[10] and theoretically[11] proposed. Theoretical studies based on the distribution function theory were applied also to the problem on the Stokes shifts and succeeded in explaining not only the Stokes shift[12] but also the dynamic Stokes shift.[13]

However the experimentally observed absorption bandwidths cannot be directly compared with the theoretical predictions on the solvent fluctuation. Under the structureless spectra there are vibrational structures obscured by the large solvent fluctuation. It is in general difficult to separate the bandwidth into the intramolecular vibrational and the intermolecular solvent contributions.[14] It is often assumed that the solvent does not drastically change the intramolecular contribution, and the intramolecular contribution is extracted from the spectra in nonpolar solvents such as alkanes neglecting the solvent contribution. However, since the solvent can alter the electronic structure of the solute, the intramolecular contribution can in principle change with solvents.

It is important to investigate the solvent effect on the absorption bandwidth including the change in the electronic structure of a solute. In this work we have studied both the absorption spectrum and the resonance Raman spectrum of a solvatochromic dye molecule dissolved in liquids and fluids

[⊗] Abstract published in *Advance ACS Abstracts,* November 15, 1997.

S1089-5639(97)01310-8 CCC: $14.00

SCHEME 1: Phenol Blue (PB): (a) Ground State (Neutral Form), (b) Excited State (Charge-Separated Form)[a]

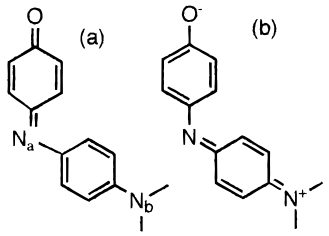

[a] The marks "a" and "b" are used to distinguish the position of the isotope substitution.

from near the critical to the liquidlike densities using so-called supercritical fluids. Resonance Raman study is considered to be suitable for this purpose, since the vibrational modes strongly coupled to the optical transition make large contributions to both absorption and resonance Raman spectra.[14] We have chosen phenol blue (PB, Scheme 1) as a probe molecule. PB is a well-known solvatochromic dye and its absorption band maximum is often used as a solvent parameter.[15] It has a well-separated absorption band in the visible region (around 600 nm), whose position moves from blue to red as the polarity or the hydrogen donating ability of the solvents increases. PB is considered to have a "neutral" form (Scheme 1a) in its ground state and a "charge-separated" form (Scheme 1b) in its excited state. These two forms constitute resonance structures, and the contribution of the "charge-separated" form is expected to increase as the solvent polarity or the hydrogen donating ability increases, which was assured by semiempirical molecular orbital (MO) calculations by Warshel et al.[16] and by Zerner et al.[17] As is shown later, such a change in the electronic structure is also observed in the resonance Raman spectra, which indicates that the solvent dependence of intramolecular vibrational modes should be taken into account.

We have measured the spectra in a variety of solvents, ranging from protic solvents such as ethylene glycol to nonpolar solvents such as ethane at the density near to its critical density. We consider that the so-called supercritical fluids are suitable for the study of the solvent effects, since we can change the density continuously to gaseous one where the solvent effects are small. In addition, the fluids near the gas−liquid critical points have unique characters both in static and dynamic properties as represented by the local density enhancement. Such characters of the supercritical fluids currently attract interests in a wide field of chemistry, both academic and industrial.[18] Vibrational spectroscopy has also been applied to the study of the solute−solvent interaction in such a density region, but mainly by means of IR spectroscopy.[19] Most studies on fluids in the medium-density region by the Raman spectroscopy have been restricted to the solvent properties,[20−23] or small-size solute molecules such as hydrogen,[24] iodomethane,[25,26] or acetone,[27] due to the low solubilities of ordinary organic molecules and the low sensitivity of the Raman spectroscopy, although the study on naphthalene in CO_2 has been done in the higher density region.[28] In this work, we have developed a new high-pressure optical cell which is suitable for the resonance Raman spectroscopy, and studied how the solvent density affects the vibrational structure of a large organic molecule.

We have measured the absorption and the resonance Raman spectra of PB, and analyzed comprehensively the solvent dependence of the following five quantities: absorption peak shift, absorption bandwidth, resonance Raman peak shift, resonance Raman intensity and resonance Raman bandwidth. Absorption peak is the averaged energy difference between the ground and the excited states. Absorption bandwidth reflects the transition energy fluctuation induced by the solvent, and the intramolecular nuclear structure change on excitation which is included as vibrational progressions. Raman Stokes shift is the strength of intramolecular chemical bonds, which is determined by the electronic structure of the ground state. Resonance Raman intensity is a measure of the intramolecular structural change on excitation (although excitation profile of absolute cross section is desirable, we only measured the relative intensities at single excitation energy for experimental reasons). Raman bandwidth reflects the magnitude and modulation frequency of vibrational frequency induced by solvent fluctuation. These five quantities and the relationships among them will be discussed in detail.

This paper consists of six sections. In section 2 we briefly review the theoretical basis to discuss the band shape of the absorption spectrum and the intensity of the resonance Raman spectrum, the Raman bandwidth, and the connection with solvent properties. Section 3 is the experimental section. Experimental results are given in section 4. A tentative assignment based on the ^{15}N isotope shift and vibrational spectra of related species is proposed there. Section 5 is the discussion, and concluding remarks are given in section 6.

2. Theoretical Basis of Analysis

2.1. Electronic Absorption Spectrum. We consider the model where both intramolecular vibrational modes and the solvent fluctuation are expressed as harmonic oscillators coupled to the electronic transition from the ground to the excited state.[29] The harmonic oscillator is characterized by three quantities: the vibrational frequency ω, the dimensionless displacement Δ, and the magnitude of the frictional force on it. Intramolecular modes are usually high frequency ($\omega \gg k_BT$) and underdamped (low friction), whereas solvent modes are low frequency ($\omega \ll k_BT$) and overdamped (high friction). The displacement is also expressed in terms of reorganization energy $\lambda = \omega\Delta^2/2$. In our model, the intramolecular vibrational mode is represented by a single oscillator with the frequency of ω_v, and the reorganization energy of λ_v. In the Brownian oscillator model the solvent fluctuation is described by a single (or several) classical harmonic oscillator, whose properties are characterized by two parameters: the solvent reorganization energy λ_s and the correlation time Λ^{-1}. We assume here that the relaxation of the solvent is much slower than the optical dephasing time $(2k_BT\lambda_s)^{-1/2}$ (static limit), since a large solvent reorganization energy is expected for broad and structureless spectra[30] (Figure 4). In such a model, the absorption spectrum is expressed as[31]

$$\epsilon(\omega) \propto \omega I_A(\omega)$$

$$I_A(\omega) = \frac{\exp(-\lambda_v/\omega_v)}{\sqrt{4\pi k_B T\lambda_s}} \sum_{n=0}^{\infty} \frac{(\lambda_v/\omega_v)^n}{n!} \exp\left[-\frac{\{\omega-(\lambda_s+\Delta G+n\omega_v)\}^2}{4\lambda_s k_B T}\right] \quad (1)$$

where $\epsilon(\omega)$ denotes the molar extinction coefficient, and $I_A(\omega)$ is the line shape function of the absorption spectrum. ΔG is the energy gap between the bottoms of the ground and the excited states. In the static limit, the band shape due to the solvent contribution corresponds to the static distribution function of the transition energy itself (which is described as a Gaussian), and the whole spectrum is a vibrational progression convoluted with the solvent contribution. The first-order and the second-order cumulants, ω_0 and σ^2, respectively, are given by

$$\omega_0 = \Delta G + \lambda_s + \lambda_v \tag{2}$$

$$\sigma^2 = 2k_B T\lambda_s + \omega_v\lambda_v \tag{3}$$

which stand for the center and the squared width of the spectrum, respectively. The lifetime effect on the absorption bandwidth is considered to be negligible in the present case.[32]

In our model there are only two parameters which characterize the solvent effect, that is, the mean transition energy ω_0 and the solvent reorganization energy λ_s. Our principal interest is how the solute−solvent and the solvent−solvent interactions affect the observed spectra. In principle it is desirable to know the relation between the solvent reorganization energy and the intermolecular specific interactions at the molecular level. However, the dielectric continuum model of solvents is often useful for an order estimation, especially when the electronic transition is accompanied with a large change in charge distribution. Under such an approximation the absorption peak shift and the solvent reorganization energy are, for example, expressed as follows[33]

$$\delta\omega_0 = \frac{\mu_g^2 - \mu_e^2}{4\pi\epsilon_0 a^3}\frac{n^2-1}{2n^2+1} + \frac{2\mu_g(\mu_g - \mu_e)}{4\pi\epsilon_0 a^3}\left(\frac{\epsilon-1}{\epsilon+2} - \frac{n^2-1}{n^2+2}\right) \tag{4}$$

$$\lambda_s = \frac{(\mu_e - \mu_g)^2}{4\pi\epsilon_0 a^3}\left(\frac{\epsilon-1}{\epsilon+2} - \frac{n^2-1}{n^2+2}\right) \tag{5}$$

Here the dipole moments of the ground and the excited states are denoted as μ_g and μ_e, respectively. $\delta\omega_0 = \omega_0(\text{gas}) - \omega_0(\text{solution})$ is the mean peak shift from the absorption peak without solvent to that in solution. The radius of the dielectric cavity (which corresponds to the distance of the center of solute and solvent molecules) is a. ϵ and n^2 are the zero frequency and optical frequency dielectric constants, respectively. The first term of eq 4 corresponds to the contribution from the solvent electronic polarizability, and the second term arises from the nuclear reorientational motion. The former immediately responds to the electronic transition, and does not show the additional reorganization, whereas the reorganization energy of the latter is given by eq 5. If we neglect the first term in eq 4, the following linear relationship between the peak shift and the reorganization energy holds,

$$\delta\omega_0 : \lambda_s = -2\mu_g : \mu_e - \mu_g \tag{6}$$

2.2. Resonance Raman Spectrum. The resonance Raman scattering is a two-photon process; a molecule is first excited by the excitation photon, then the nuclear wave packet propagates on the excited state potential surface, and finally the molecule returns to the ground state by emitting the scattered photon. The intensity of each vibrational band is determined by two factors, that is, Albrecht A-term and B-term.[34] The former is the nuclear wave function overlap of the final state with the wave packet of the initial state after the time development on the excited state surface. The latter is the nuclear coordinate dependence of the transition dipole moment. Usually A-term dominates the spectrum under the resonance condition. When the optical dephasing is fast, the time development of the nuclear wave packet is determined by the slope of the Franck−Condon region of the excited-state potential surface. In such a case, the relative intensity is given by[14,35]

$$\sigma_R(\omega_L,\omega_S) \propto \omega_L\omega_S^3\omega_v\lambda_v \tag{7}$$

where σ_R is the scattering cross section, ω_L and ω_S are the frequencies of the excitation laser and the scattered photon, respectively. We have assumed that ω_v of the excited state is the same as that of the ground state. Equation 7, together with eq 3, means that the intramolecular vibrational modes of strong Raman bands (vibrational modes with large reorganization energy) give large contributions to the bandwidth of the absorption spectrum. We can also infer the structure of the excited state from the resonance Raman spectrum, since the nuclear displacement on the transition is related to the reorganization energy.

The band shape of the Raman spectrum is the Fourier transform of the time correlation function of the Raman scattering tensor, and its width is determined by the vibrational and the rotational relaxation.[36] We neglect here the rotational relaxation, since our probe molecule PB is such a large molecule that the rotational relaxation is expected to be much slower than the vibrational one. The vibrational relaxation is usually dominated by the pure dephasing. In the stochastic formalism dephasing mechanism is divided into two, homogeneous and inhomogeneous broadenings.

In the homogeneous case the rate of the frequency modulation Λ is larger than the inverse of the root-mean-squared fluctuation $\langle|\delta\omega|^2\rangle^{1/2}$ (fast modulation). In such a case the Raman band shape is a Lorentzian, and fwhm (full width at half-maximum) of the Raman band $\Delta\nu_{1/2}$ is[36]

$$\Delta\nu_{1/2} = 2\langle|\delta\omega|^2\rangle/\Lambda \tag{8}$$

The Raman band becomes narrower as the modulation becomes faster, because the frequency fluctuation is averaged, which is called "motional narrowing".

In the inhomogeneous case where the solvent modulation is slower than the inverse of the root-mean-squared fluctuation, the Raman band shape is a Gaussian and its fwhm is[36]

$$\Delta\nu_{1/2} = 2\sqrt{2\ln 2\langle|\delta\omega|^2\rangle} \tag{9}$$

The solvent fluctuation is frozen here, and the observed band shapes represent the distribution of the vibrational frequency, as in the case of the absorption spectrum. In both cases, of course, the Raman bandwidth is larger when the magnitude of the frequency fluctuation is larger, although its dependence on the frequency fluctuation is different.

3. Experiment

3.1. Materials. PB-^{14}N (Aldrich 97%) is purified twice by recrystallization from ethyl acetate-ligroine 1:1 mixture. Further purification by alumina column[37] did not alter the observed spectra. We prepared two types of isotope substituted PB; PB-$^{15}N_a$ and PB-$^{15}N_b$ (for the position of the substituted nitrogen, see Scheme 1). The preparation method is as follows (Scheme 2); Aniline *N*-methylation was performed by the reaction with formaldehyde and sodium borohydride in sulfuric acid.[38] Then nitroso group was introduced at para position by the usual method. *p*-Nitrosodimethylaniline was reduced by sodium borohydride to p-Dimethylphenylenediamine,[39] from which PB was prepared by the method proposed by Vittum et al.[40] Crude dyes were purified by alumina column.[37] Isotope sources, aniline-^{15}N and sodium nitrite-^{15}N, were purchased from Isotec Inc. (^{15}N 99%). Sample production was assured from the absorption, the resonance Raman and the IR spectra.

All liquid solvents were purchased from Nacalai Tesque and used as received. CO_2 (Sumitomo Seika, >99.99%), CF_3H

SCHEME 2: Reaction Scheme of the Synthesis of PB

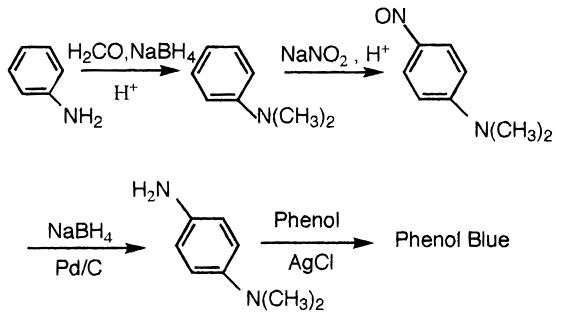

(Asahi Glass, >99.999%), N_2O (Seitetsu Kagaku, >99.99%) and C_2H_6 (Sumitomo Seika, >99%) were used without further purification.

3.2. Apparatus. The 514.5 nm line of an argon ion laser (Cyonics, 10mW) was used as the excitation light in resonance Raman experiments. The scattering at 90° was collected and focused onto the slit of a 60 cm single spectrograph (Engis, Model 600). A holographic filter (Kaiser, Super Notch Plus) was placed in front of the slit. Signal was detected by an intensified silicon photodiode array (EG&G, Model 1421) and stored in a personal computer. Spectral resolution was about 4 cm^{-1}. Wavenumber calibration was performed by measuring the Raman spectra of solvents with known frequencies (toluene and acetone). Detector sensitivity was calibrated by measuring the fluorescence of quinine.[41] Sample concentrations were controlled so as to obtain the best signal-to-noise ratios.

In measuring the resonance Raman band with broad band absorption, it is quite important to reduce both the absorption of the laser beam before the scattering position and the reabsorption of the scattering light by the sample. They are crucial especially in the measurement of supercritical fluid solutions where the sample cell is required to stand for high pressure. To accomplish this aim, we have designed a new high-pressure optical cell of a simple design with which a number of spectroscopic measurements such as absorption, fluorescence, transient absorption, and Raman spectroscopies can be made by changing the optical windows. In designing we referred to the optical cell designed by Jodl and Holzapfel for the high-pressure Raman measurement at low temperatures.[42] Figure 1 shows the cross section of the high-pressure Raman cell used for the measurement. The cell is made of titanium and can be used at least up to 50 MPa. The optical cell is equipped with four windows, three of them are used for the Raman measurement: one for the laser input, another for the laser output, and the last one for the scattering light. The laser beam was introduced into the cell through a pinhole of 2 mm diameter and reflected at 90° by a prism attached to the optical window (BK-7). The distance between the edge of the prism and the optical window for the scattering was set to be as small as possible, in order for the laser beam to pass through the cell nearest to the optical window. This reduces both the absorption of the laser beam before the scattering position and the reabsorption of the scattering light by the sample solution. The aperture of the optical window for the scattering light was taken to be large (1.9 of f-value). Special care was taken to get rid of stray light and wall scattering as possible as we could.

In the measurement a proper amount of solid sample was placed in the cell, and the cell was purged by a fluid in use. The optical cell is connected to the reservoir of the high-pressure fluid by a 1/16-in. capillary tube, and the fluid is introduced from the reservoir. The sample was dissolved within the cell by a magnetic stirrer. Temperature was controlled within ±0.5K by flowing thermostated water through the cell. The pressure

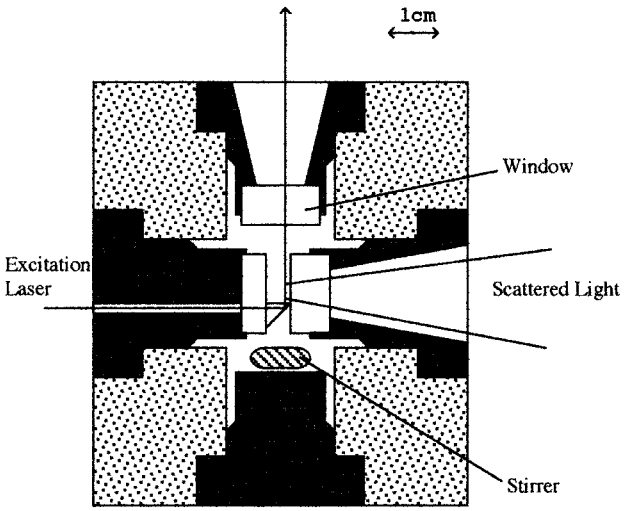

Figure 1. The cross section of the high-pressure optical cell. See details in the text.

was measured by a stainless gage (Kyowa, PGM 500KH), and the densities of the fluids were calculated by empirical equations of states.[43] All experiments were performed at the reduced density ρ_r (density divided by the critical density ρ_c) larger than 1.0 due to the low solubility of PB in fluids.

All experiments on liquid solution spectra were performed at room temperature. Spectra in supercritical fluids were measured at 50 °C. We have also measured the temperature effect on the CF_3H solution at 10 °C. Absorption spectra were measured by a multichannel photodetector (Otsuka Electronics, MCPD-2000). Absorption spectra at pressures higher than 30 MPa were measured by using a different optical cell[44] and a spectrometer (Shimadzu, UV 2500PC). No concentration effect was found in the observed spectra. Long time laser exposure did not alter the observed Raman spectra.

4. Results

4.1. Absorption spectra. Absorption spectra of PB are shown in Figure 2. The absorption peak wavelength λ_{max} agrees with the previously reported value.[15,45,46] It can be easily noticed that λ_{max} shifts from blue to red with increasing the solvent polarity or the hydrogen donating ability. On the other hand, the absorption bandwidth is almost the same in liquid solvents, which contradicts to the theoretical prediction (eq 6) that λ_s increases in proportion to $\delta\omega_0$. Interesting is the behavior in fluids that the widths are much larger than those in liquids although the peak shifts are smaller, as easily noticed by comparing the spectra in fluids with that in cyclohexane (Figure 2, lower panel).

We have fitted these spectra to eq 1 to estimate the first and the second-order cumulants, ω_0 and σ,[2] respectively. In the fitting procedure, the intramolecular vibrational frequency ω_v was fixed at 1500 cm^{-1}. Examples of the fittings are shown in Figure 3. Although the deviation of the simulation is found on the blue edge, we consider it is mainly due to the overlap with the S_0-S_2 absorption, and that the bandwidth calculated from this fitting does not deviate largely from the real value. In the case of such structureless spectra, division of the bandwidth to the intramolecular part and the solvent part is in general difficult. We indeed found some uncertainty in the division. However, the summation of the two contributions stayed within ±20 cm^{-1}.

The parameters ω_0 and σ^2 are correlated in Figure 4. In liquid solvents virtually no correlation is found, although a slight

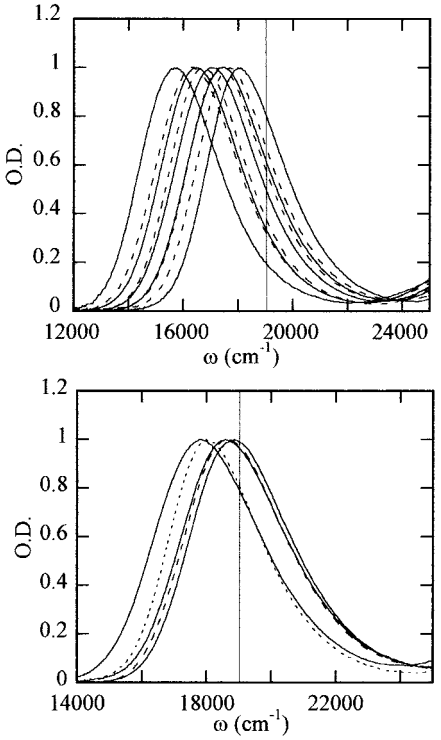

Figure 2. Absorption spectra of PB. Upper: spectra in liquid solvents at room temperature; from left to right, in ethylene glycol, methanol, dimethyl sulfoxide (DMSO), chloroform, acetonitrile, benzene, ethyl acetate, carbontetrachloride, cyclohexane. Lower: spectra in supercritical fluids at 323.2 K. From left to right, in CF_3H (2.00), CO_2 (1.90), N_2O (1.98), ethane (2.00). Their reduced densities are written in parentheses. The spectrum in cyclohexane is drawn by the dotted curve for reference. Excitation energy for the resonance Raman measurement is indicated by the vertical lines.

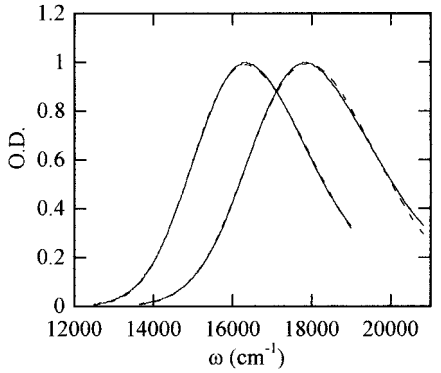

Figure 3. Examples of the fitting of the absorption spectra; left: in methanol, right: in CF_3H (2.00). The observed and the fitted spectra are drawn by the solid and the broken lines, respectively.

increase of σ^2 with a decrease of ω_0 is found. In supercritical fluids, however, σ^2 is significantly larger than those in liquid solvents. Furthermore, σ^2 decreases almost linearly as the solvent density increases. All of these phenomena violate the linear relationship between the peak shift and the bandwidth (eq 6). However, comparing the spectra in various supercritical fluids at the same reduced density, σ^2 increases with decreasing ω_0 as is expected from the solvent polarity. It is possible that the different thermal energy (50 °C) in supercritical fluids may bring about apparent broadening of the absorption spectrum, since the solvent fluctuation contribute to the bandwidth as $\lambda_s k_B T$(eq 3). To check this effect, we have measured the spectrum in CF_3H at 10 °C. Lowering the temperature of course sharpened the spectra, but the bandwidths of the CF_3H solutions at 10 °C were still larger than those of liquid solutions. This

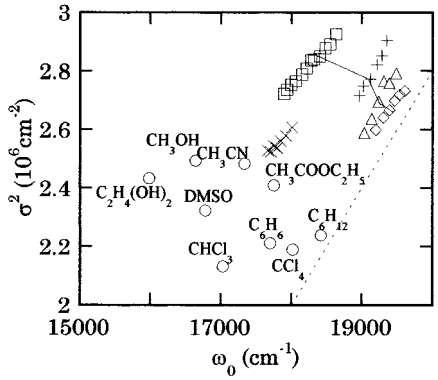

Figure 4. The relation between the first-order (ω_0) and the second-order (σ^2) cumulants of absorption spectra. ○, in liquid solvents; □, in CF_3H (1.00∼2.57) at 50 °C; ×, in CF_3H (2.20∼2.80) at 10 °C; +, in CO_2 (1.00∼1.90); △, in N_2O (1.00∼1.98); ◇, in ethane (1.00∼2.00). In each supercritical fluid, ω_0 is smaller at the higher density. Data points in supercritical fluids at $\rho_r = 1.60$ are united by the solid line. The dotted line is explained in section 5.

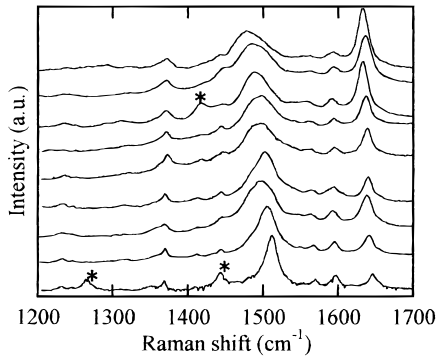

Figure 5. Resonance Raman spectra in liquid solvents; from upper to lower, in ethylene glycol, methanol, DMSO, chloroform, acetonitrile, benzene, ethyl acetate, carbontetrachloride, cyclohexane. Solvent bands are marked with *.

means that σ^2 is really larger in fluids than in liquids with similar values of ω_0 at the same temperature.

The absorption bandwidth contains both the intramolecular and the solvent contributions, as mentioned before. When the electronic structure depends on solvents, the intramolecular contribution is also expected to vary with solvents. Such a change should be reflected in the resonance Raman spectra, so we will return to the problem of the absorption bandwidth in section 5 after the examination of the resonance Raman spectra.

4.2. Resonance Raman Spectra. Resonance Raman spectra of PB in liquid solvents and in supercritical fluids are shown in Figures 5 and 6, respectively. Solvent bands in the spectrum of the ethylene glycol solution were subtracted since a strong solvent band overlaps with the C═N stretching band of PB (described below). The spectra drastically change with solvents and solvent densities. No fluorescence due to PB was observed at least around 560 nm, where the Raman bands were observed.[47]

We first try to assign each vibrational mode to discuss the origin of these solvent dependent peak shifts and bandwidths, since this is the first study on the vibrational spectra of PB. For assignment we prepared two ^{15}N substituted species, PB-$^{15}N_a$ and PB-$^{15}N_b$ (Scheme 1). Their resonance Raman spectra in carbontetrachloride, acetonitrile and methanol are shown in Figure 7 together with those of PB-^{14}N. It is easily noticed that the Raman band around 1500 cm^{-1} (whose position strongly depends on solvents) shows a large isotope shift in PB-$^{15}N_a$, which clearly indicates that this band is the C═N stretching mode. The strong band around 1640 cm^{-1}, whose frequency

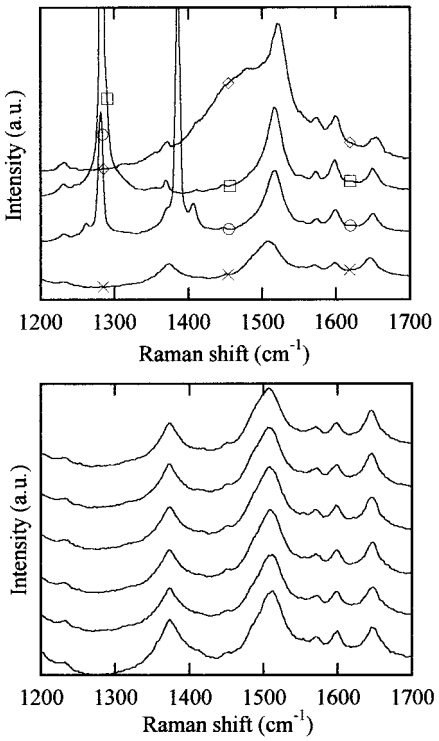

Figure 6. Resonance Raman spectra of PB in various solvent fluids and at various densities. (a) Spectra at $\rho_r = 1.60$ (except for CF_3H solution at $\rho_r = 1.61$) and 323.2 K. From upper to lower, in C_2H_6, N_2O, CO_2, CF_3H. (b) Spectra in CF_3H at various densities. From top to bottom: $\rho_r = 1.03$, 1.22, 1.41, 1.61, 1.80, and 2.00 at 50 °C.

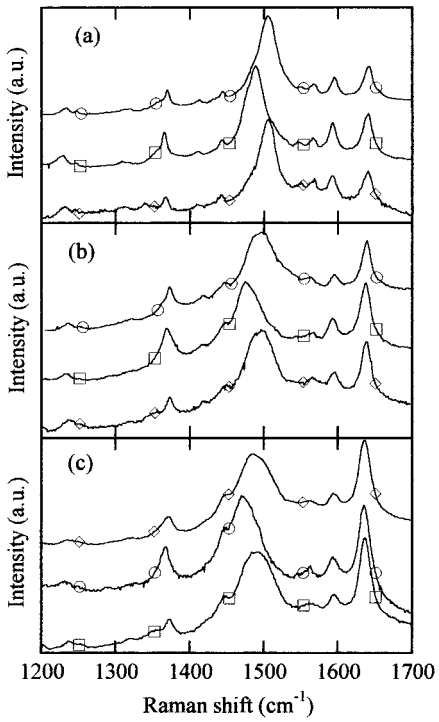

Figure 7. ^{15}N isotope shifts of Raman bands. Each spectrum is obtained in (a) carbontetrachloride, (b) acetonitrile, and (c) methanol, respectively. From upper to lower, PB-^{14}N, PB-$^{15}N_a$, PB-$^{15}N_b$.

shifts largely, is assigned to the carbonyl C═O stretching mode, since we have observed a strong band at nearly the same position in the FT-IR spectra measured in KBr. A small band around 1560 cm^{-1}, which also shows a low-frequency shift with increasing the solvent polarity, is assigned to the C═C symmetric stretch of the quinone ring. The frequencies of the above-mentioned three modes decrease with increasing the solvent polarity, as is expected by the electronic structure changes from the neutral to the charge separated forms (Scheme 1).

TABLE 1

frequency in CCl_4 (cm^{-1})				
PB-^{14}N	PB-$^{15}N_a$	PB-$^{15}N_b$	intensity[a]	assignment
1641	1641	1641	s	C═O str
1596	1593	1593	m	DMA 8a[b]
1568	1566	1566	m	C═C sym str
1550	1546	1549	w	
1505	1488	1505	vs	C═N_a str
~1480	*c*	~1480	sh	
1445	1443	1542	m	$\delta^s(CH_3)$
1412	1411	1409	w	?[d] $\delta^a(CH_3)$
1371	1365	1367	m	
~1355	~1355	1339	m	ring-N_b str
1315	1313	1311	w	
1247	1245	1245	w	
1235	1229	1232	m	?[d] ring−N_a str

[a] vs, very strong; s, strong; m, medium; w, weak; sh, shoulder. [b] The mode that corresponds to the 8a mode of DMA. [c] Not observed. [d] Tentative assignments.

Between the C═O and the C═C stretching modes a band of medium strength is found (near 1600 cm^{-1}) which shows a slight red shift with decreasing the electronic transition energy. We assigned this band to the 8a vibration of the dimethylaniline (DMA) part of the PB (hereafter called 8a), because of the similarity of this frequency to the 8a mode of DMA (1605 cm^{-1}).[48] Since the DMA part of the PB in its charge separated form (Scheme 1) resembles the DMA cation radical, the solvent shift also follows the change of the vibrational shift from DMA to its radical cation. In fact, the frequency of the 8a mode in DMA cation radical is reported as 1568 cm^{-1},[49] whose shift relative to the band of DMA is consistent with our experimentally observed shift of the corresponding mode.

Only a small change is found on the substitution of amino-nitrogen (PB-$^{15}N_b$, Figure 7). Most significant change was found in the band near 1370 cm^{-1} in PB-^{14}N, which consists of sharp and broad components. In PB-$^{15}N_b$, the broad component moves to the lower frequency and the sharp one remains. This broad component is considered to be the N_b-ring stretch. The corresponding band of DMA lies near, 1348 cm^{-1},[48] which supports this assignment. Our assignments, including tentative ones for bands not mentioned in the text, are summarized in Table 1.

In the following, we will mainly discuss the peak position and bandwidth of the C═O and the C═N stretching modes which show large solvent dependence. The peaks, the widths and the intensities of Raman bands were determined by fitting the bands to a Gaussian after the baseline (determined from polynomial fit) was subtracted. Examples of the fitting are shown in Figure 8. The low-frequency side of the C═N stretching mode was omitted in the fitting, since a shoulder was found here. In methanol, DMSO and ethylene glycol we could not fit the whole band shapes of the C═O stretching mode by a single Gaussian function, and we used the summation of two Gaussian functions with the same peak frequency.

Figure 9 shows the correlation between the absorption band center and the vibrational frequency shifts of the C═N stretching and the C═O stretching modes. Both bands show large shifts with increasing the solvent polarity or the hydrogen donating ability in a variety of solvents, and with increasing solvent density in supercritical fluids. Good correlation is found in both bands, which indicates that the ground-state electronic structure has some correlation with the transition energy. The density dependence in supercritical fluids is also in correlation with the absorption band center as in the solvent dependence within liquid

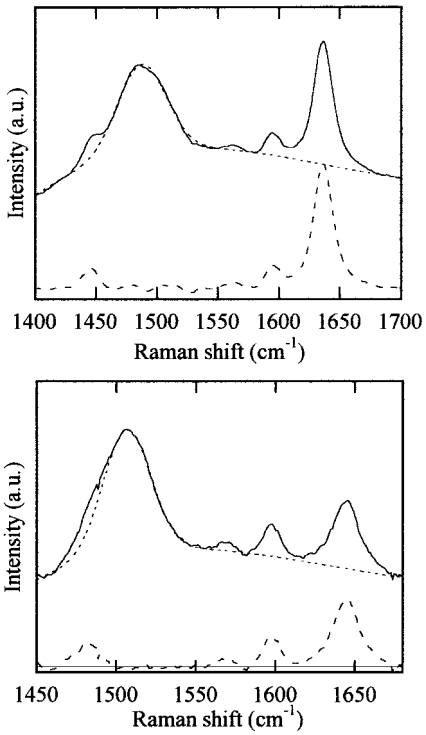

Figure 8. Examples of the fitting of C═N Raman bands: upper, in methanol; lower, in CF_3H (1.61). The observed and the fitted spectra are drawn by the solid and the dotted lines, respectively. The residue of the fit is drawn by the broken lines.

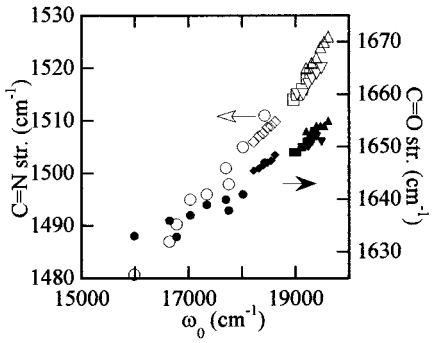

Figure 9. Raman band shifts of the C═N stretching and the C═O stretching modes. ○, C═N in liquid solvents; ◇, C═N in CF_3H (1.03∼2.00); □, C═N in CO_2 (1.00∼1.90); ▽, C═N in N_2O (1.00∼1.98); △, C═N in ethane (1.00∼2.00); ●,C═O in liquid solvents; ◆, C═O in CF_3H; ■, C═O in CO_2; ▼, C═O in N_2O; ▲, C═O in ethane.

solvents. This means that the solvent density effect on the frequency of the C═N stretching and the C═O stretching modes can be explained in terms of the effect on the transition energy, as in the case of the solvent effect in liquid solvents.

As is shown in Figures 5 and 6, the bandwidth of the C═N stretching band is not only relatively large in comparison with other bands but also shows large solvent dependence. Figure 10 shows the plot of the bandwidth of the C═N stretching modes obtained by the spectral fitting against the absorption band center. The bandwidth of the C═O stretching mode was almost constant irrespective of the solvent, and are smaller than that of the C═N stretching mode. We should at first examine the possibility that the broad band we assigned to the C═N stretching mode is actually composed of several bands due to other vibrational modes whose widths are not broad. In fact the obtained bandwidths for PB-^{14}N are larger than those for PB-$^{15}N_a$ in acetonitrile and methanol. We consider this is due to the shoulder peak observed in the case of PB-^{14}N, which is totally hidden by the C═N stretching band in the case of PB-

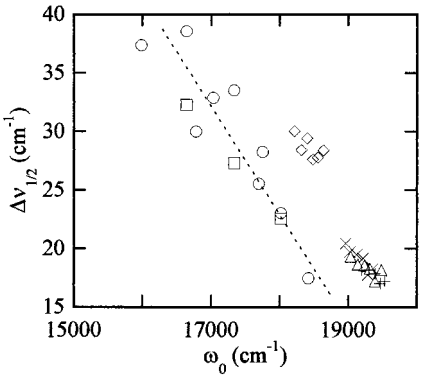

Figure 10. The bandwidths of the C═N stretching mode against the absorption band center. ○, in liquid solvents; □, PB-$^{15}N_a$ in methanol; acetonitrile and carbontetrachloride; ◇, in CF_3H (1.00∼2.57); ×, in CO_2 (1.00∼1.90); △, in N_2O (1.00∼1.98); +, in ethane (1.20∼2.00).

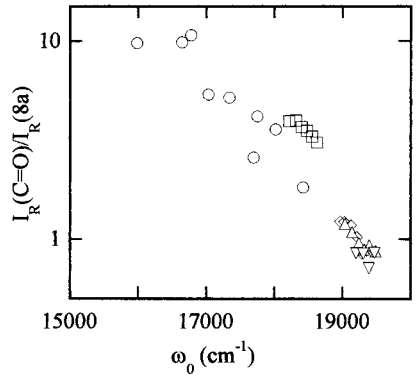

Figure 11. The relative intensity ratio of the C═O stretching and the 8a modes against the band center. Longitudinal axis is drawn in logarithmic scale. ○, in liquid solvents; □, in CF_3H (1.03∼2.00); ◇, in CO_2 (1.00∼1.90); △, in N_2O (1.00∼1.98); ▽, in ethane (1.40∼2.00).

$^{15}N_a$. However, the width is still large in the case of PB-$^{15}N_a$, where the effect of the overlap is small. Furthermore, the width is small in nonpolar solvents (such as cyclohexane and CCl_4), and the band does not seem to suffer from the overlap with other bands. Therefore, we conclude that the width of the C═N stretching band is indeed large, although we may slightly overestimate the bandwidth of PB-^{14}N. As is shown in Figure 10, a fairly good linear relationship between the absorption band center and the C═N bandwidth is found, if we compare the bandwidths in liquid solutions only. This suggests that the origin of the broadening of the bandwidth is the same as that of the peak shift of the absorption band. This point is discussed in detail in section 5. It is to be noted that the bandwidths are larger in fluids than in liquid solvents if compared at the same transition energy, as found in the absorption bandwidth.

The intensity of the resonance Raman band is an important quantity in considering the bandwidth of the absorption spectrum. It can be easily noticed from Figures 5 and 6 that the relative intensity of each band also depends on solvents. In particular the C═O stretching band grows as the absorption peak shifts to red. Figure 11 shows the relative intensity of the C═O stretch and the 8a against the absorption band center. We have chosen these bands, because they are strong in all solvents, separated from other resonance and solvent bands, and so close to each other that reabsorption correction is not required. In the plot, we show the relative intensity by a log scale. The relative intensity in all solvents used here has good correlation with the absorption band center, although the results of the CF_3H solution have a somewhat large deviation.

The Raman intensity consists of two contributions, one is the nuclear coordinate displacement on excitation (Albrecht

A-term), and the other is the vibronic interaction (B-term). If the former dominates the band intensity, which is usual in the resonance condition, the change in the relative intensity means that the intramolecular vibrational reorganization energy changes with the solvent. To check the assumption, we have measured the spectra of several liquid solutions excited by a krypton ion laser (647 nm).[55] The relative intensity of the C═O band was slightly smaller in the Kr^+ excited spectra. Since the excitation energy is fixed in our experiments, the relative position in the absorption spectrum moves to red as the absorption peak moves blue. Even if we admit that the change in the relative intensity shown in Figure 11 is partly explained from the B-term contribution, the solvent dependence was much larger than the excitation energy dependence. We also measured the depolarization ratio in CCl_4 solution. The values were close to 1/3, which is the characteristic value of the A-term enhancement. Therefore the B-term contribution is considered to be minor in this case.

5. Discussion

We summarize the experimental results briefly as follows. (a) The center of the absorption band ω_0 does not correlate with the bandwidth σ^2 (Figure 4), in contradiction to the linear correlation between ω_0 and λ_s predicted by the dielectric continuum model (eq 6). (b) The peak shift and the relative intensity of the resonance Raman band correlate well with ω_0 (Figures 9 and 11). (c) The widths of the absorption spectrum and the C═N stretching band in supercritical fluids do not correlate with those in liquid solvents.

To discuss the origin of the above-mentioned phenomena, we first investigate the electronic structures of the ground and the excited states, since they determine the vibrational reorganization energy λ_v, which is another source of absorption bandwidth (eq 3). Resonance Raman spectra can be used for this purpose, and we will discuss it in section 5.1. The Raman bandwidth is discussed in connection with the absorption bandwidths in 5.2. At first sight, the result (c) seems to reflect the character of the density fluctuation in fluids in the medium-density region, which has been extensively discussed in the absorption and fluorescence peak shifts.[18] However, our result can be explained without invoking such an enhanced fluctuation, based on the discussion in section 5.1 and 5.2. Finally, the solvent density dependence of the solvent fluctuation will be discussed in 5.3 in connection with its molecular origins.

5.1. The Origin of the Anomalous Absorption Bandwidths in Liquids. The large solvent dependence of the resonance Raman spectra of PB can be considered to reflect the electronic structure change of PB induced by solvents. Provided that the resonance between the neutral and the charge separated forms (Scheme 1) is enhanced in polar solvent as mentioned in section 1, it will weaken the C═N, C═O, and C═C bonds, which can explain their solvent shifts. In principle, the vibrational frequency of polar bonds can shift in polar solvents, even if the electronic structure does not change.[50] However, considering the large magnitude of the shift, especially that of the C═N stretching mode, and the change of the relative Raman intensities, the electronic structure change of the solute is likely to be the main cause for the shift.

The vibrational frequency shifts due to the electronic structure change were in fact found previously in other species.[51,52] For example, Spiro et al. showed that in the case of *N*-methylacetamide (NMA) the frequency and strength of the resonance Raman bands assigned to the C−N and the C═O stretching modes change with solvents.[51] They explained the behavior using the Hückel MO method. Recently Markham et al. applied an ab initio calculation to NMA$(H_2O)_3$ cluster and obtained the spectrum close to the experimentally observed one in water.[53] We consider that vibrational frequency shifts due to the electronic structure change are not so rare, and that our observation is another example.

The problem is the way the solute−solvent interaction affects the spectra. It is well-known that the absorption peak shift of PB is not correlated with the dielectric constants, and depends on both the solvent polarity and the hydrogen donating ability.[15] Although both effects lower the transition energy, their mechanisms are different from each other; the former works on the solute as a whole such as a reaction field, whereas the latter works almost exclusively on the oxygen atom. If the hydrogen donating ability is reflected on the electronic structure, we should be able to observe it in the resonance Raman spectra. For example, we can expect the peak shift of the C═O stretching band to be larger in protic solvents. However, no meaningful difference can be found between the effects of polar and protic solvents on the peak shift and the relative intensity of the Raman spectra (Figures 5, 6, and 9). This means that whatever the interaction brings about the shift of the absorption spectrum, the structural changes for both the ground and the excited states are characterized by only one parameter, ω_0. We consider that this behavior is originated in the electronic structures of PB, which is easily changed by its environment as expressed by the resonance structure, although further theoretical studies are needed to ascertain this point.

The next question is how the structural changes discussed above manifests itself in the absorption bandwidth. The resonance Raman intensity is an important quantity in this regard, since the stronger Raman bands contributes more to the absorption bandwidth as is represented by eqs 3 and 7. As shown in Figure 11, the relative intensity ratio of the 8a and the C═O stretching modes strongly depends on solvents, which indicates the possible change of the intramolecular contribution to the absorption spectrum. Unfortunately we could not experimentally determine the relative values of λ_v among different solvents, since we could not obtain the excitation profiles of the absolute cross section with our equipment. A simple resonance consideration, however, predicts that λ_v decreases with decreasing ω_0, because the ground and the excited states become more similar to each other as they mix. Figueras found that the transition dipole moment increases as the transition energy decreases.[15] It means that the overlap of wave functions of both states increases, which also supports our consideration.

On the basis of the above argument, we have tried to divide σ^2 into the contributions of λ_v and λ_s by simply assuming that $\omega_v\lambda_v$ is a linearly increasing function of ω_0, and that λ_s is nearly equal to zero in alkanes such as cyclohexane and ethane. The assumption is not necessarily strict, since the solvent density may also contribute to the reorganization as is discussed later. However the contribution of the density is expected to be smaller than that of the electric multipoles. The dotted line in Figure 4 shows the relation of $\omega_v\lambda_v$ with ω_0 obtained under the above assumptions, explicitly given by

$$\omega_v\lambda_v = 400\omega_0 - 5\,200\,000 \qquad (10)$$

In drawing this line, the coefficients are chosen to give a parallel line to the line which connects σ^2 in ethane at $\rho_r = 1.0$ and cyclohexane, and to give a small portion of λ_s (ca. 100 cm^{-1}) in these solvents. The value of λ_s in various solvents can be calculated by subtracting $\omega_v\lambda_v$ estimated by eq 10 from σ^2 in eq 3. The estimated λ_s is shown against ω_0 in Figure 12. We obtain a fairly good correlation between ω_0 and λ_s estimated

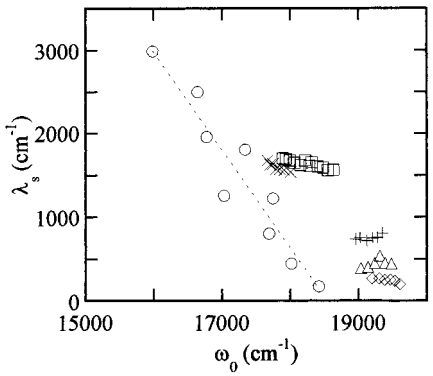

Figure 12. An estimate of the solvent reorganization energy. All marks are the same as Figure 4.

in this way, and the order of λ_s in liquid solvents is comparable to the values reported for other solvatochromic dye systems.[10] The tendency of the larger λ_s with the larger absorption peak shift is also reasonable, since generally a large-energy difference between two states accompanies large rearrangements or reorientational dynamics of the solvents. The values of λ_s for supercritical fluids still deviates from this correlation, which is the same situation as is observed in $\Delta\nu_{1/2}$ for the C═N stretching mode. We will discuss this point in section 5.3. It is interesting that almost a linear correlation between ω_0 and λ_s is obtained as is expected from the dielectric continuum model given by eq 6. If we simply apply this relation, μ_e/μ_g is estimated as 3.4. However, it is to be noted that the estimated λ_s in liquid solvents are not necessarily correlated well with the dielectric constants as predicted by eq 5, as is the case of the spectral shift.

5.2. The Width of the C═N Raman Band. The bandwidth of the Raman spectrum is determined by the fluctuation of the vibrational frequency (eqs 8 and 9), which stems from the thermal motions of solvents. We found that the bandwidth of the C═N stretching mode is extraordinarily large and shows peculiar solvent dependence. It will be interesting to investigate the origin of the width in connection with the absorption bandwidth, which also originates from the solvent fluctuation.

The bandwidth is determined by two quantities, the magnitude and the speed of the vibrational frequency modulation (eqs 8 and 9). The large bandwidth of the C═N stretching mode means that either $\delta\omega$ is larger or Λ is smaller for the C═N bond. We think the former more probable, since the very large solvent dependence of the frequency of the C═N stretching mode suggests that its frequency easily changes with environment. As is shown in Figure 9, the transition energy shift and the C═N peak shift are strongly correlated. This means that the fluctuation of the transition energy should lead to the fluctuation of the C═N frequency. The former appears in the absorption bandwidth as λ_s, and the latter contributes to the Raman bandwidth of the C═N stretching band as discussed above. It is quite natural that there is a good correlation between λ_s and $\Delta\nu_{1/2}$ within this argument, and this is confirmed by the similarity between Figures 10 and 12. From the same consideration, the width of the C═O stretching band is also expected to be large. However, the width of the C═O stretching band is not so large as that of the C═N stretching mode, although it is slightly larger than those of other bands. We consider that it is due to the smaller solvent dependence of the vibrational frequency of the C═O stretching mode.[54]

Motional narrowing can also modify the solvent dependence of the Raman bandwidth. Since the solvent with large band shift, such as ethylene glycol, has larger viscosity than nonpolar solvents such as cyclohexane, the Raman spectra may be broadened by the slow relaxation (eq 8). However, the correlation with the solvent viscosity is not so good in the present case. We consider that the main reason is $\delta\omega$, although the solvent dependence may be enhanced by the motional narrowing.

In general the solvent fluctuation which appears in vibrational spectra is different from the fluctuation which determines the absorption bandwidth. The vibrational bandwidth comes mainly from the collisional interaction, whereas the absorption bandwidth stems from the long-range electrostatic interaction. However, we cannot explain the anomalous Raman bandwidth of the C═N stretching band from the collisional interaction. The hydrogen bonding can broaden the bandwidth, for N_a is another possible hydrogen accepting site. But the effect should be larger on the C═O stretching band. Considering the similarity between Figures 10 and 12, the main part of the C═N bandwidth is likely to arise from the fluctuation of the electronic transition energy. We in fact found that the Raman Stokes shift of the C═N stretching mode depends on the excitation energy in polar or protic solvents, which can be the evidence of the correlation of the both fluctuation.[54,55]

5.3. The Origins of the Solvent Induced Absorption Peak Shift and the Bandwidth. The remaining problem is the relatively large solvent fluctuation in fluids compared with that in liquid solvents, as is represented in Figures 10 and 12. To begin with, we consider the reason the nonpolar solvent cyclohexane gives the absorption peak shift as large as CF_3H. The shift of ω_0 in cyclohexane from that of isolated PB vapor is about 2000 cm^{-1}, if we estimate the ω_0 of isolated PB from the zero-density extrapolation of the density dependence in ethane. Such a large shift is not limited to the case of PB. Solvatochromism of 2-nitroanisole (π^*-value) in supercritical fluids has been well-studied,[56] and cyclohexane is known to give a large shift as supercritical solvents whose dielectric constants are much larger than that of cyclohexane. This indicates that the solute specific interaction is not the reason for the large absorption peak shift of PB in cyclohexane.

In recent years, it has been demonstrated that a substantial amount of the solvation energy arises from multipole interactions even in nondipolar solvents. Maroncelli et al. studied the fluorescence Stokes shift of Coumarin 153, and they showed that the solvent with a large quadrupole or an octapole moment gives rise to a large fluorescence Stokes shift even if it has no dipole moment.[10] Cyclohexane, however, does not have any large higher order multipole moment, and Maroncelli et al. classified it to a genuine nonpolar solvent. The large solvent shift of PB in cyclohexane does not arise from the reorientation of the solvent.

According to eq 4, the transition energy shift is divided into the contributions from the electronic polarizability and the solvent reorientation. The former is often neglected in the discussion on the liquid solution since the solvent dependence of the polarizability is much smaller than the multipole interaction. On the other hand, supercritical solvents as a whole have small polarizabilities compared with liquid solvents[57] (their low critical temperature means the weak solvent−solvent attractive interaction, substantial amount of which arises from the dispersion force). We consider the absorption peak shift in CF_3H is for the most part due to the solvent reorientation, whereas that in cyclohexane arises from the solvent polarizability.

This difference in the origin of the absorption peak shift between cyclohexane and CF_3H can also explain their difference in the bandwidth of both the absorption and the resonance Raman spectra. According to the dielectric continuum theory,

the fluctuation due to the dipolar reorientation accompanies the reorganization energy, while the polarization contribution does not. In our assumption, the absorption peak shift in CF_3H is for the most part due to the solvent reorientation, whereas the absorption peak shift in cyclohexane arises from the solvent polarizability. The former has the corresponding reorganization energy whereas the latter not, which can cause the difference in the solvent reorganization energy, i.e., the absorption bandwidth.

Although we consider that the difference in solvent polarizability is the principal reason for the difference between liquid and supercritical solvents, there still remains a question if the electronic polarizability does not contribute to the reorganization energy in supercritical fluids. At the molecular level, the absorption band shift is proportional to the solvent polarization multiplied by the solvent density within the range of the electrostatic interaction (we neglected here the effect of the local field). If the solvent density around the solute fluctuates, a genuine nonpolar solvent can also cause the corresponding transition energy fluctuation.[58,59] Since the fluctuation of the bulk density is large in fluids near the critical point, the density fluctuation around the solute also seems large in the medium-density region. On the other hand, the density fluctuation seems small in the high-density region since molecules are closely packed here. Although the solvent density fluctuation around a solute is sometimes discussed in terms of compressibility (the fluctuation of the bulk solvent density), we know only a few studies in which it was actually examined in supercritical fluids. These results indicate that the density fluctuation around a solute is not always proportional to the solvent compressibility.[60−62] Solvent density fluctuation around a solute is a remaining problem to be studied in the future.

6. Conclusion

We have for the first time measured the resonance Raman spectra of PB in various solvents, ranging from protic solvents such as ethylene glycol to nonpolar supercritical solvents such as ethane near their critical densities. We have found that the C═N and the C═O stretching bands show large solvent shifts, reflecting the solvent dependence of the electronic structures of PB. Their shifts are correlated well with the absorption peak shift, irrespective of the solute−solvent interaction specificity. The relative intensities of the Raman bands also change with solvents and are correlated with the absorption peak shift. Both relations stand for the correlation of the ground and the excited electronic structures with the transition energy shift. We further found that the bandwidth of the C═N stretching mode broadened with the red shift of the absorption. The width is, however, larger in supercritical solvents compared with that in liquid solvents at the same absorption peak.

We have also measured the bandwidth of the absorption spectrum, the solvent dependence of which is at first sight very confusing. In liquid solvents it apparently has no correlation with the absorption peak shift. In fluids the width is larger than in liquid solvents, and it increases with a decrease of the solvent density. This anomaly is ascribed to the change of the intramolecular vibrational reorganization energy due to solvents, since the electronic structure changes with solvents. We subtracted the intramolecular contribution from the absorption bandwidth by simply assuming linear dependence of the intramolecular reorganization energy on the electronic transition energy. The estimated solvent reorganization energies are reasonable within liquid solvents and also correlated with the Raman bandwidth of the C═N stretch mode. The narrow bandwidth in liquids is originated in the large polarizabilities which brings the transition energy shift without fluctuation. Solvent density dependence of the fluctuation of the number of solvents around a solute should be clarified in order to realize the density dependence of bandwidths in fluids.

Acknowledgment. We thank Mr. F. Amita (Kyoto University) for constructing the optical cell for the resonance Raman measurement in high-pressure fluids. We are grateful to Dr. Y. Yoshimura (Kyoto University) for his help in the measurement of the absorption spectra at the pressure higher than 30 MPa.

References and Notes

(1) See, e.g., Reichardt, C. *Solvents and Solvent effects in Organic Chemistry*; VCH: Weinheim, 1988.

(2) (a) Gould, I. R.; Noukakis, D.; Goodman, J. L.; Young, R. H.; Farid, S. *J. Am. Chem. Soc.* **1993**, *115*, 3830. (b) Gould, I. R.; Noukakis, D.; Gomez-Jahn, L.; Young, R. H.; Goodman, J. L.; Farid, S. *Chem. Phys.* **1993**, *176*, 439.

(3) Kjaer, A. M.; Ulstrup, J. *J. Am. Chem. Soc.* **1987**, *109*, 1934.

(4) Cortés, J.; Heitele, H.; Jortner, J. *J. Phys. Chem.* **1994**, *98*, 2527.

(5) (a) Reid, P. J.; Barbara, P. F. *J. Phys. Chem.* **1995**, *99*, 3554. (b) Johnson, A. E.; Levinger, N. E.; Jarzeba, W.; Schlief, R. E.; Kliner, D. A. V.; Barbara, P. F. *Chem. Phys.* **1993**, *176*, 555. (c) Walker, G. C.; Akesson, E.; Johnson, A. E.; Jevinger, N. E.; Barbara, P. F. *J. Phys. Chem.* **1992**, *96*, 3728. (d) Akesson, E.; Walker, G. C.; Barbara, P. F. *J. Chem. Phys.* **1991**, *95*, 4188.

(6) (a) Tominaga, K.; Kliner, D. A. V.; Johnson, A. E.; Levinger, N. E.; Barbara, P. F.; *J. Chem. Phys.* **1993**, *98*, 1228. (b) Walker, G. C.; Barbara, P. F.; Doorn, S. K.; Dong, Y.; Hupp, J. T. *J. Phys. Chem.* **1991**, *95*, 5712.

(7) (a) Wynne, K.; Gailli, C.; Hochstrasser, R. M. *J. Chem. Phys.* **1994**, *100*, 4797. (b) Wynne, K; Reid, G. D.; Hochstrasser, R. M. *J. Chem. Phys.* **1996**, *105*, 2287.

(8) (a) Markel, F.; Ferris, N. S.; Gould, I. R.; Myers, A. B. *J. Am. Chem. Soc.* **1992**, *114*, 6208. (b) Kulinowski, K.; Gould, I. R.; Myers, A. B. *J. Phys. Chem.* **1995**, *99*, 9017. (c) Kulinowski, K.; Gould, I. R.; Ferris, N. S.; Myers, A. B. *J. Phys. Chem.* **1995**, *99*, 17715.

(9) Zerg. Y.; Zimmt, M. B. *J. Phys. Chem.* **1992**, *96*, 8395.

(10) Raynords, L.; Gerdecki, J. A.; Frankland, S. J. V.; Horng, M. L.; Maroncelli, M. *J. Phys. Chem.* **1996**, *100*, 10337.

(11) Perng, B.-C.; Newton, M. D.; Raineri, F. O.; Friedman, H. L. *J. Chem. Phys.* **1996**, *104*, 7153.

(12) Perng, B.-C.; Newton, M. D.; Raineri, F. O.; Friedman, H. L. *J. Chem. Phys.* **1996**, *104*, 7177.

(13) Hirata, F.; Munakata, T.; Raineri, F.; Friedman, H. L. *J. Mol. Liq.* **1995**, *65/66*, 15.

(14) (a) Myers, A. B. *Chem. Phys.* **1994**, *180*, 215; (b) Myers, A. B. *Chem. Rev. (Washington, D.C.)* **1996**, *96*, 911.

(15) Figueras, J. *J. Am. Chem. Soc.* **1971**, *93*, 3255.

(16) Luzhkov, V.; Warshel, A. *J. Am. Chem. Soc.* **1991**, *113*, 4491.

(17) Karelson, M. M.; Zerner, M. C. *J. Phys. Chem.* **1992**, *96*, 6949.

(18) See, e.g., Savage, P. E.; Gopalan, S.; Mizan, T. I.; Martino, C. J.; Brock, E. E. *AIChE J.* **1995**, *41*, 1723.

(19) See, e.g., Poliakoff, M.; Howdle, S. M.; Karaian, S. G. *Angew. Chem., Int. Ed. Engl.* **1995**, *34*, 1275.

(20) Garrabos, Y.; Chandrasekharan, V.; Echargui, M. A.; Marsault-Herail, F. *Chem. Phys. Lett.* **1988**, *160*, 697.

(21) Ben-Amtoz, D.; LaPlant, F.; Shea, D.; Gardecki, J.; List, D. *ACS Syp. Ser.* **1992**, *488*, 18.

(22) Salmoun, F.; Dubessy, J.; Garrabos, Y.; Marsault-Herail, F. *J. Raman. Spectrosc.* **1994**, *25*, 281.

(23) Okazaki, S.; Matsumoto, M.; Okada, I.; Maeda, K.; Kataoka, Y. *J. Chem. Phys.* **1995**, *103*, 8594.

(24) Howdle, S. M.; Bagratashvili, V. N. *Chem. Phys. Lett.* **1993**, *214*, 215.

(25) Fan, R.; Kalbfleisch, T.; Ziegler, L. D. *J. Chem. Phys.* **1996**, *104*, 3886.

(26) Ziegler, L. D.; Fan, R. *J. Chem. Phys.* **1996**, *105*, 3984.

(27) Akimoto, S; Kajimoto, O. *Chem. Phys. Lett.* **1993**, *209*, 263.

(28) Zerda, T. W.; Song, X.; Jonas, J. *Appl. Spectrosc.* **1986**, *40*, 1194.

(29) See, e.g. Mukamel, S. *Principles of Nonlinear Optical Spectroscopy*; Oxford University press: New York, 1995.

(30) Li, B.; Johnson, A. E.; Mukamel, S.; Myers, A. B. J. *Am. Chem. Soc.* **1994**, *116*, 11039.

(31) Marcus, R. A. *J. Phys. Chem.* **1989**, *93*, 3078.

(32) We have totally neglected the lifetime (T_1) effect on the absorption bandwidth in our model. We have performed transient absorption measurements on PB in several solvent fluids. Since we could not detect the transient absorption spectrum due to the excited state clearly, we could not obtain the lifetime of the excited state directly. The ground-state recovery shows decay with two time constants; near the center of the absorption peak, the

first component is about 0.3 ps, and the slow one is nearly 10 ps in methanol. The fast component depends on the solvent and has a tendency to become larger as the absorption peak shift blue. According to these results, it is probably safe to say that the lifetime of the excited state (T_1) is no shorter than 0.3 ps. The T_1 effect on the bandwidth is of the order $(2\pi cT_1)^{-1}$, which is smaller than 20 cm^{-1}. Since the total width σ is larger than 1000 cm^{-1}, we can safely neglect the T_1 effect.

(33) McRae, E. G. *J. Phys. Chem.* **1957**, *61*, 562.

(34) Albrecht, C. A. *J. Chem. Phys.* **1961**, *34*, 1476.

(35) Heller, E. J.; Sundberg, R. L.; Tannor, D. *J. Phys. Chem.* **1982**, *86*, 1822.

(36) See, e.g. Rothchild, W. G. *Dynamics of Molecular Liquids*; Wiley: New York, 1984.

(37) Kolling, O. W.; Goodnight, J. L. *Anal. Chem.* **1973**, *45*, 160.

(38) Guimanini, A. G.; Chiavari, G.; Musiani, M. M.; Rossi, P. *Synthesis* **1980**, 743.

(39) Nelson, T.; Wood, H. C. S.; Wylie, A. G. *J. Chem. Soc.* **1962**, 371.

(40) Vittum, P. W.; Brown, G. H. *J. Am. Chem. Soc*. **1946**, *68*, 2235.

(41) Hamaguchi, H.; *Appl. Spec. Rev.* **1988**, *24*, 137.

(42) Jodl, H. J.; Holzapfel, W. B. *Rev. Sci. Instrum.* **1979**, *50*, 340.

(43) (a) Huang, F. H.; Li, M. H.; Lee, L. L.; Starling, K. E.; Chung, F. T. H. *J. Chem. Eng. Jpn.* **1985**, *18*, 490. (b) Rubio. R. G.; Zollweg, J. A.; Streett, W. B. *Ber. Bunsen-Ges. Phys. Chem.* **1989**, *93*, 791. (c) Couch, E. J.; Hirth, L. J.; Kobe, K. A. *J. Chem. Eng. Data* **1961**, *6*, 229. (d) Younglove, B. A.; Ely, J. F. *J. Phys. Chem. Ref. Data* **1987**, *16*, 577.

(44) Kimura, Y.; Yoshimura, Y.; *J. Chem. Phys.* **1992**, *96*, 3824.

(45) Kim, S.; Johnson, K. P. *AIChE J.* **1987**, *33*, 1603.

(46) Kim, S.; Johnson, K. P. *Ind. Eng. Chem. Res.* **1987**, *26*, 1206.

(47) Very weak fluorescence emission usually means very short lifetime at the excited state. However, we do not consider that it contradicts with our estimate of the excited-state lifetime T_1 no shorter than 0.3 ps.[32] According to our discussions in section 5.1, solvent reorganization energies are smaller than 3000 cm^{-1}, which leads to the pure dephasing time T_2 longer than 20 fs. The ratio of the intensities of fluorescence and Raman is estimated by $(2T_1/T_2)$.[29] Therefore the fluorescence should be about 30 times stronger than the Raman emission. However, we consider it reasonable that we did not detect the fluorescence emission for the following two reasons. First, the fluorescence spectrum is expected to be very broad as the absorption spectrum. Therefore, the fluorescence will be very weak compared with the Raman emission even if it is 30 times greater when integrated over the whole spectrum region. Second, the large solvent reorganization energy naturally leads to the large fluorescence Stokes shift. Considering the mirror image relationship between the absorption and the fluorescence spectra, the fluorescence spectrum will appear in the near-infrared region, far from the region where we observed the Raman spectrum.

(48) Guichard, V.; Buorkba, A.; Lautie, M. F.; Poizat, O. *Spectrochim. Acta* **1989**, *45A*, 187.

(49) Poizat, O.; Guichard, V.; Buntiinx, G.; *J. Chem. Phys.* **1989**, *90*, 4697.

(50) For example, the frequency of the C≡N stretching mode of CH_3CN varies about 13 cm^{-1} from gas phase to neat liquid (Ben-Amotz, D.; Meng-Rong, L.; Cho, S. Y.; List, D. J. *J. Chem. Phys.* **1992**, *96*, 8781).

(51) Wang, Y.; Purrello, R.; Georgiou, S.; Spiro, T. G. *J. Am. Chem. Soc.* **1991**, *113*, 6368.

(52) Musilli, M. M.; Loppnow, G. R. *Chem. Phys. Lett.* **1996**, *261*, 691.

(53) Markham, L. M.; Hudson, B. S. *J. Phys. Chem.* **1996**, *100*, 2731.

(54) Yamaguchi, T.; Kimura, Y.; Hirota, N. In preparation.

(55) Yamaguchi, T.; Kimura, Y.; Hirota, N. *J. Chem. Phys.* **1997**, *107*, 4436.

(56) Yonker, C. R.; Frye, S. L.; Kalkwalf, D. R.; Smith, R. D. *J. Phys. Chem.* **1986**, *90*, 3022.

(57) Besserer, G. J.; Robinson, D. B. *J. Chem. Eng. Data*, **1973**, *18*, 137

(58) Matyushov, D. V.; Schmid, R. *J. Chem. Phys.* **1995**, *103*, 2034.

(59) Matyushov, D. V.; Schmid, R. *Mol. Phys.* **1995**, *84*, 533.

(60) Kalbfleisch, T. S.; Ziegler, L. D.; Keyes, T. *J. Chem. Phys.* **1996**, *105*, 7034.

(61) Yoshimura, Y. *Mol. Phys.* **1995**, *86*, 1419.

(62) Stephens, M. D.; Saven, J. G.; Skinner, J. L. *J. Chem. Phys.* **1997**, *106*, 2129.